

Extended States in the Bandgap, Local Field Enhancement, Bidirectional Reflection Zeros, and Ideal Broadband Superluminal Tunneling in PT-symmetric EM Structures

Amir M. Jazayeri

*The College of Optics and Photonics (CREOL), University of Central Florida, Orlando, FL, USA
amir@ucf.edu*

We introduce novel band-structure concepts in non-Hermitian non-tight-binding electromagnetic (EM) structures with PT symmetry (without P and T symmetries separately), and examine certain novel phenomena thereof. The phenomena include (i) the emergence of what we name ‘extended states in the bandgap’ as the dual of the well-known ‘bound states in the continuum’, (ii) the enhancement of the EM fields at specific frequencies within specific regions, which is especially important in combination with nonlinear effects to be examined later, (iii) ‘bidirectional’ reflection zeros, which is atypical of structures with PT symmetry but without P and T symmetries, and (iv) superluminal tunneling, which is ‘ideal’ in the sense that the transmission coefficient has a uniform phase and unit magnitude over a broad bandwidth while reflection is zero.

Introduction.– The purpose of this Letter is to introduce the band-structure concept of ‘fixed points’ (viz., points on the band structure which remain intact if certain parameters change), and examine the resulting novel phenomena in PT-symmetric non-Hermitian electromagnetic (EM) structures. The phenomena to be reported are (i) the enhancement of the EM fields at specific frequencies within specific regions, which might find applications, especially in combination with nonlinear effects, (ii) the emergence of what we name ‘extended states in the bandgap’ as the dual of the well-known ‘bound states in the continuum’ [1-5], (iii) reflection zeros which are bidirectional, and are therefore atypical of structures with PT symmetry but without P and T symmetries [6], and (iv) ‘ideal’ superluminal tunneling as tunneling with zero reflection and with a transmission of uniform phase and unit magnitude over a broad bandwidth, whereas in the superluminal-tunneling phenomena reported so far, the reflection coefficient is not zero, and the magnitude of the transmission coefficient is usually very small [7-11]. It is noteworthy that any superluminal-tunneling effect [10-13] is in fact a combination of two phenomena which do not necessarily accompany each other; tunneling as the transmission of a considerable amount of energy through a barrier [14], and superluminal behavior as an unusually small group delay [7-9,15-18].

Relevant Symmetries & Models.– Before turning to the main purpose of this Letter, let us briefly review the significance of T and P symmetries in physics, and refer to a few models which might seem similar to the EM structures to be examined in this Letter. For a time-independent spin-less Hamiltonian H , the T (viz., time reversal) symmetry condition reads $H^* = H$ in real space, and $\hat{H}^*(-\vec{k}) = \hat{H}(\vec{k})$ in momentum (or quasimomentum) space, where the asterisks denote complex conjugation. In two spatial dimensions, electronic systems without T symmetry are allowed to support topologically-protected edge states [19-21], whose EM

counterpart can be found in structures of materials with non-reciprocal EM response [22]. By adding spin degrees of freedom, electronic systems with T symmetry are allowed to support symmetry-protected edge states [23-25], whose EM counterpart has been realized by the use of ring resonators [26] and bi-anisotropic media [27], where the role of spin is played by propagation direction and polarization, respectively.

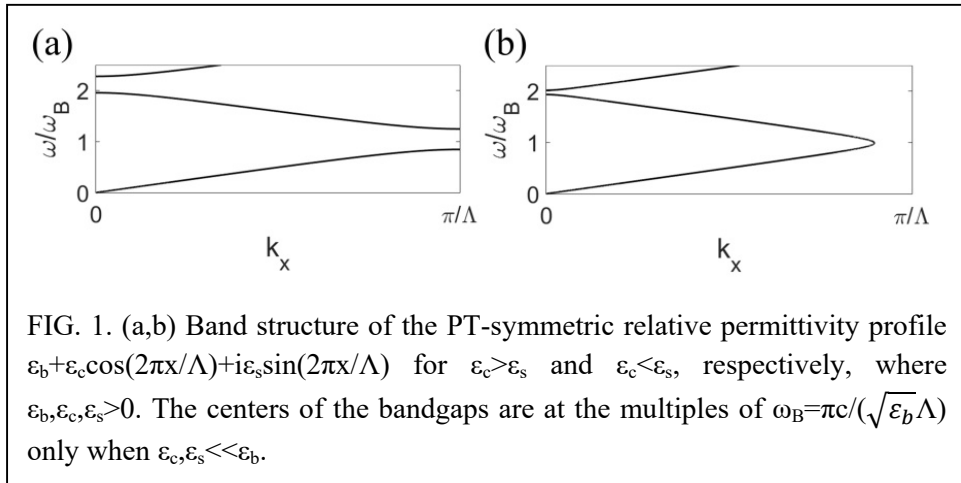
On the other hand, P (viz., parity inversion) is the reversal of either one coordinate axis or the three coordinate axes all. The reversal of two coordinate axes is also sometimes called parity inversion, although it is in fact a π -rotation. Unlike the T operator, which is always non-Hermitian, always anti-unitary (leading to $TiT^{-1} = -i$), and sometimes non-involutory (viz., T^{-1} and T are sometimes different), the P operator (and the π -rotation operator) is always Hermitian, unitary, and involutory.

PT symmetry (viz., the composition of P and T symmetries) is especially important in non-Hermitian systems. For instance, the SSH model [28] has two well-known non-Hermitian versions; one which respects PT symmetry [29,30], and the other which does not [29,31]. Non-Hermiticity in the latter, which does *not* respect PT symmetry, completely changes the topological character of the original SSH model [29,31], and also leads to a fundamental difference between the energy spectrum calculated under periodic boundary conditions and the one calculated under open boundary conditions [29,31] *however large* the length of the open sample is chosen.

Another consequence of PT symmetry is that the eigenvalues of a PT-symmetric non-Hermitian Hamiltonian may be all real in a parameter range [32]. The parameter value at which some (or all) of the eigenvalues start to become complex is called an exceptional point. However, it should be noted that PT symmetry is not the only symmetry which allows non-Hermitian Hamiltonians to have real eigenvalues. For instance, the non-Hermitian version of the SSH model which does not respect PT symmetry *does* have real energy spectra in certain parameter ranges, but, due to lack of PT-symmetry, its energy spectrum and exceptional points depend on the choice of boundary conditions.

Regarding the EM counterpart of the SSH model, its non-Hermitian versions, or some other tight-binding electronic models, it should be noted that they are usually realized by an array of parallel waveguides weakly coupled to each other, where the propagation constant along the waveguides plays the role of energy in the corresponding electronic model [33-36]. Therefore, the resulting EM realization is in fact ‘inexact’ in the sense that the resulting EM band structure and group velocity (whether defined based on the relation between the EM frequency and the propagation constant along the waveguides, or between the EM frequency and the Bloch wavenumber perpendicular to the waveguides) are *not* equivalent to the band structure and group velocity in the corresponding electronic model.

Let us now look into a PT-symmetric *non-tight-binding* EM model, which was first examined in [37]. The underlying refractive index profile of the EM model reads $n_b + n_c \cos(2\pi x / \Lambda) + i n_s \sin(2\pi x / \Lambda)$ in the frequency domain, where $0 < n_c, n_s \ll n_b$. The structure examined in [37] is in fact a finite length of this refractive index profile within $x = 0$ and $x = w = M\Lambda$ in a background of the refractive index n_b , where M is a positive integer. It is evident that an incident wave may see a structure starting with loss or gain depending on its propagation direction. At a certain excitation frequency, let us write the reflected and transmitted electric fields as $\hat{y}R_L \exp(-in_b k_0 x)$ and $\hat{y}T_{LR} \exp(in_b k_0 (x - w))$ when the structure is illuminated from the left at $x = 0$ by the incident electric field $\hat{y} \exp(in_b k_0 x)$, and as $\hat{y}R_R \exp(in_b k_0 (x - w))$ and $\hat{y}T_{RL} \exp(-in_b k_0 x)$ when the structure is illuminated from the right at $x = w$ by the incident electric field $\hat{y} \exp(-in_b k_0 (x - w))$. The free-space wavenumber k_0 reads ω / c in terms of the excitation angular frequency ω . The authors of [37] observed that at the Bragg angular frequency [viz., when $\omega = \omega_B = \pi c / (n_b \Lambda)$], and for $n_s = n_c$, R_L is zero, and R_R is an unbounded and increasing function of M , whereas for $n_s = 0$, R_L and R_R both approach unity when $M \rightarrow \infty$. The unequal R_L and R_R for $n_s \neq 0$ was termed a non-reciprocal behavior in [37]. However, it should be noted that the EM structure is in fact reciprocal (viz., obeys Lorentz reciprocity), and, T_{LR} and T_{RL} are equal, and can be denoted by T . The EM structure was re-examined in [38], where the authors observed that around the Bragg frequency (viz., when $\omega \approx \omega_B$), and for $n_s = n_c$, the magnitude of T is almost unity, and its phase can be approximated by $n_b w \omega / c$ in terms of ω . In other words, for $n_s = n_c$, the structure is almost invisible (viz., acts as a medium of the refractive index n_b) when it is illuminated from the left by an incident wave packet with a frequency content around the Bragg frequency.



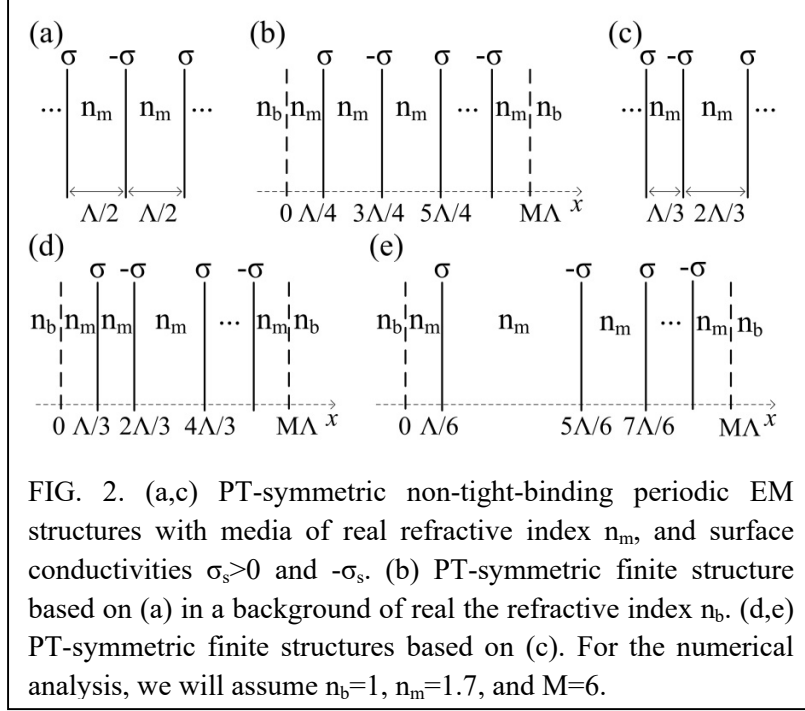
To the best of our knowledge, the non-tight-binding EM structure discussed in the previous paragraph has only been examined from the scattering-matrix viewpoint in the

literature. Therefore, it is worth looking into the band structure of its underlying periodic refractive index profile so we can later contrast its features with those of the non-tight-binding EM models to be introduced in this Letter. The refractive index profile written in the previous paragraph is equivalent to a relative permittivity profile $\varepsilon_b + \varepsilon_c \cos(2\pi x / \Lambda) + i\varepsilon_s \sin(2\pi x / \Lambda)$, where $0 < \varepsilon_c, \varepsilon_s \ll \varepsilon_b$. By using the standard Fourier expansions of the EM fields [39], we can calculate the band structure (without necessarily assuming that $\varepsilon_c, \varepsilon_s < \varepsilon_b$). As is seen in Fig. 1, for $\varepsilon_s < \varepsilon_c$, the band structure is real, and has bandgaps. The bandgap centers are at the multiples of ω_b only when $\varepsilon_c \ll \varepsilon_b$. The bandgaps all narrow as ε_s increases, and they all close when it becomes equal to ε_c , which confirms that $\varepsilon_s = \varepsilon_c$ is an exceptional point. When $\varepsilon_s = \varepsilon_c$, the band crossings are all at the multiples of ω_b (whether $\varepsilon_c \ll \varepsilon_b$ or not). When $\varepsilon_s > \varepsilon_c$, (i) the band structure is not real anymore, and k-gaps appear, and (ii) new bandgaps open. The new bandgaps are thanks to a non-zero ε_s larger than ε_c , and therefore remain open when $\varepsilon_c = 0$.

Novel Concepts & Phenomena.— We now turn to the main purpose of this Letter. We examine PT-symmetric EM structures in a category of non-tight-binding EM models, each of which has an underlying periodic permittivity profile consisting of delta functions. Such permittivity profiles, in contrast to the one leading to the band structures in Fig. 1, cannot be written in terms of a single harmonic (or even a few harmonics). Let us focus our attention on the structures depicted in Fig. 2, each of which consists of media of real refractive index n_m , and surface conductivities $\sigma_s > 0$ and $-\sigma_s$. We do not consider any surface permittivities, although the phenomena to be discussed below would still be observed if we considered small enough surface permittivities $\varepsilon_0 \varepsilon_s$ (viz., if we replaced σ_s and $-\sigma_s$ by $\sigma_s - i\varepsilon_0 \varepsilon_s$ and $-\sigma_s - i\varepsilon_0 \varepsilon_s$, respectively, where ε_0 denotes the free-space permittivity). By ‘surface conductivities’ (or ‘surface permittivities’) we mean conductivities (or permittivities) localized to regions whose widths are much smaller than the wavelength $2\pi / (n_m k_0)$. Also, we note that positive and negative surface conductivities are realizable [40,41].

Given the geometry of the EM structures depicted in Fig. 2, we use the standard transfer-matrix method [42] to analyze them at any ω . For the periodic structures [viz. those depicted in Figs. 2(a) and 2(c)], the eigenvalues of the transfer matrix relating the EM fields at $x = x_0 + \Lambda$ to the EM fields at $x = x_0$ are in fact equal to $\exp(ik_x \Lambda)$ in terms of the quasimomentum k_x (viz., Bloch wavenumber) corresponding to ω , where x_0 can be any point which does not coincide with the positions of the surface conductivities. On the other hand, for the finite structures [viz., those depicted in Figs. 2(b), 2(d), and 2(e)], we can derive the scattering-matrix elements from the transfer matrix relating the EM fields at $x = 0$ to the EM fields at $x = w = M\Lambda$. The definitions of the scattering-matrix elements (viz., the reflection coefficients R_L and R_R , and the

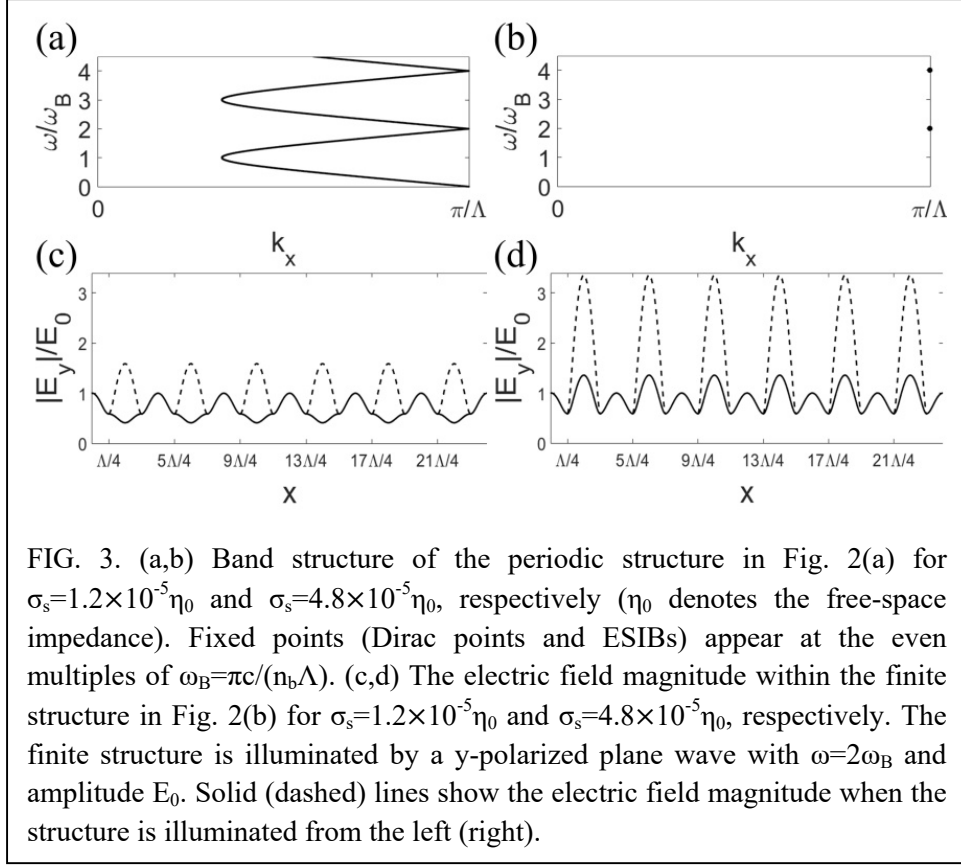
transmission coefficient T) as well as the expression of the incident wave are exactly the same as what were written in the previous section. The background refractive index n_b and the refractive index n_m will hereafter be assumed to be equal to 1 and 1.7, respectively. Also, the units of ω and σ_s will hereafter be assumed to be the Bragg angular frequency (denoted by ω_B) and the free-space impedance (denoted by η_0), respectively. We note that ω_B is equal to $\pi c / (n_m \Lambda)$ [not $\pi c / (n_b \Lambda)$] here.



As is seen in Figs. 3(a-b), the band structure of the periodic EM structure in Fig. 2(a) always has k-gaps irrespective of σ_s , and therefore has no exceptional points with respect to σ_s . When σ_s becomes larger than a threshold $\sigma_{s,TH}$ equal to $2.4 \times 10^{-5} \eta_0$, (i) the k-gaps cover the whole quasimomentum space, and (ii) a bandgap covering the whole frequency space appears.

When $\sigma_s < \sigma_{s,TH}$, there are Dirac points at the even multiples of ω_B on the band structure. When $\sigma_s > \sigma_{s,TH}$, the Dirac points turn into points we name ‘extended states in the bandgap’ (ESIB). The Dirac points and ESIB are in fact the fixed points of the band structure. The existence of such fixed points is an important feature which is absent in the band structures in Fig. 1. Given the Bloch wavenumbers equal to π / Λ at the fixed points, we expect that the electric field magnitude in the finite structure in Fig. 2(b) at any even multiple of ω_B will be periodic irrespective of the illumination direction and σ_s . This prediction is confirmed by the numerical results in Figs. 3(c-d). Interestingly, at an even multiple of ω_B , and for a certain

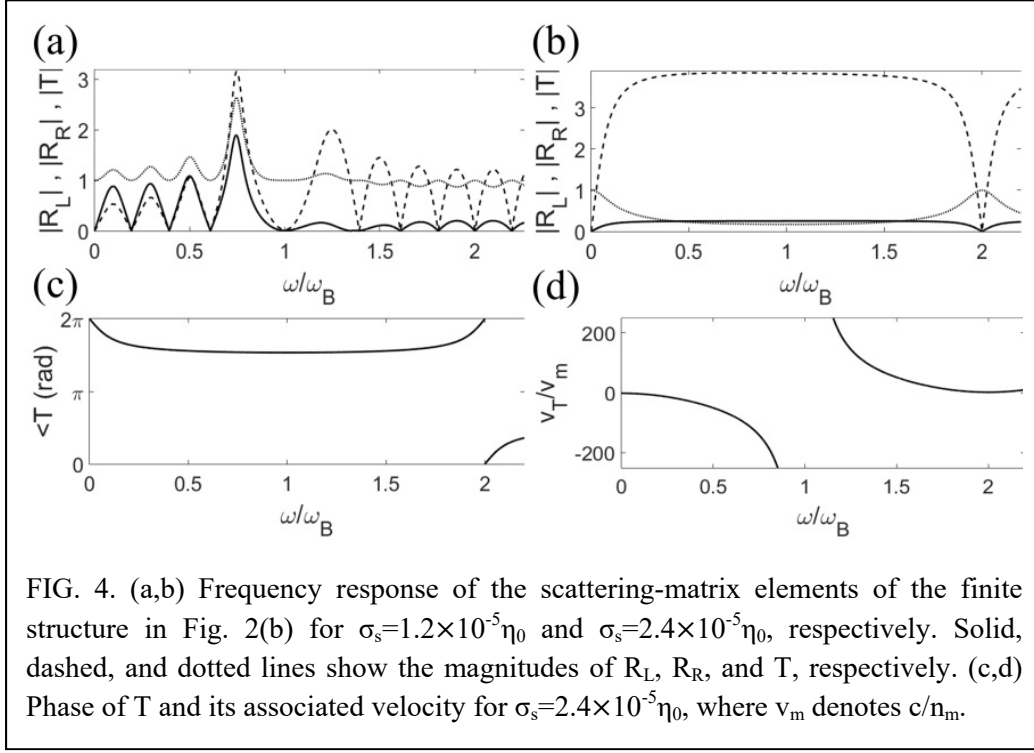
illumination direction, by increasing σ_s , the electric field magnitude remains intact within some regions of the structure while it is enhanced within other regions. Also, as is seen in Figs. 4(a-b), the reflection zeros at the even multiples of ω_B are bidirectional irrespective of σ_s .



Another important feature of the band structure in Figs. 3(a-b) for $\sigma_s < \sigma_{s,TH}$ is that the group velocity $\partial\omega/\partial k_x$ of a Bloch wave propagating from left to right (or right to left) approaches ∞ (or $-\infty$) when ω approaches any odd multiple of ω_B . Due to a jump in the Bloch wavenumbers, the group velocity is not definable exactly at the odd multiples of ω_B . However, the jump decreases when σ_s approaches $\sigma_{s,TH}$. As is seen in Fig. 4(c), when $\sigma_s = \sigma_{s,TH}$, the phase of the transmission coefficient for the finite structure in Fig. 2(b) is almost uniform around the odd multiples of ω_B , and as a result, the velocity v_T defined as $w(\partial\varphi T/\partial\omega)^{-1}$ has a very large absolute value. This superluminal tunneling at the odd multiples of ω_B is still not ideal, because (i) neither R_L nor R_R is zero, and (ii) $|T|$ is not unity.

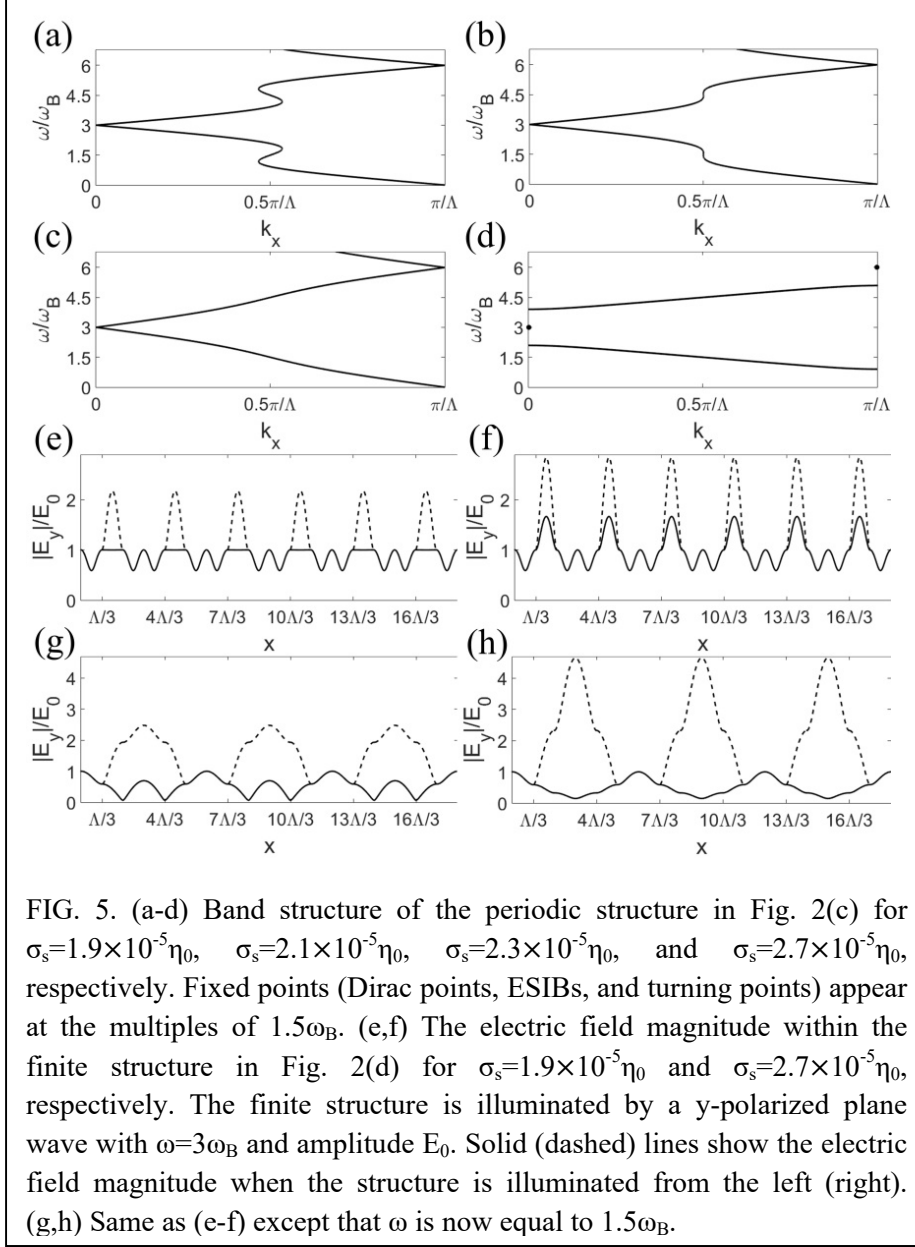
In our quest for ideal superluminal tunneling, we now examine the periodic structure depicted in Fig. 2(c) as well as its finite version depicted in Fig. 2(d). We note that the periodic structure also has another finite version depicted in Fig. 2(e). The statements to be made below

for the finite structure in Fig. 2(d) apply to the one in Fig. 2(e) as well except that the former displays a better superluminal performance.



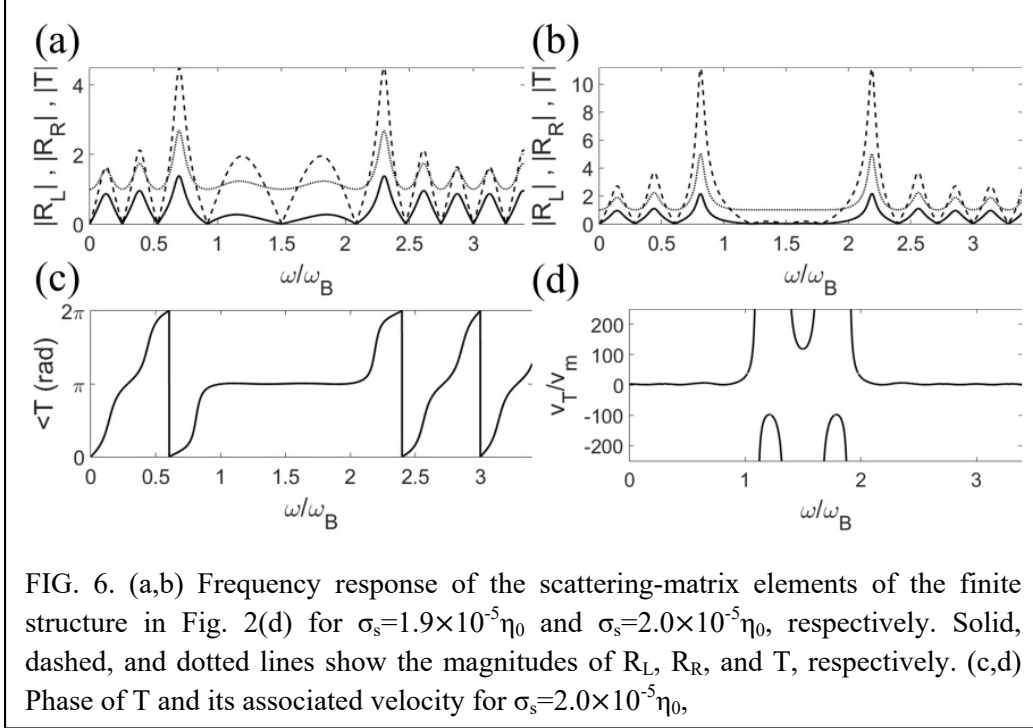
The band structure of the periodic structure in Fig. 2(c) is plotted in Figs. 5(a-d). When σ_s is smaller than a threshold $\sigma_{s,TH,1}$ equal to $2.1\times 10^{-5}\eta_0$, the band structure has k-gaps. Interestingly, the k-gaps all disappear, and the band structure becomes real when $\sigma_s > \sigma_{s,TH,1}$, contrary to the common belief that some or all eigenvalues of a non-Hermitian operator become complex when non-Hermiticity becomes large enough.

When σ_s is smaller than another threshold $\sigma_{s,TH,2}$ equal to $2.5\times 10^{-5}\eta_0$, there are Dirac points at the multiples of $3\omega_B$ on the band structure. When $\sigma_s > \sigma_{s,TH,2}$, the Dirac points turn into ESIBs. Given the Bloch wavenumbers equal to π/Λ or zero at the Dirac points and ESIBs, we expect that the electric field magnitude in the finite structure in Fig. 2(d) at any multiple of $3\omega_B$ will be periodic irrespective of the illumination direction and σ_s . This prediction is confirmed by the numerical results in Figs. 5(e-f). Also, as is seen in these figures, at a multiple of $3\omega_B$, and for a certain illumination direction, by increasing σ_s , the electric field magnitude remains intact within some regions of the structure while it is enhanced within other regions. Furthermore, as is seen in Figs. 6(a-b), the reflection zeros at the multiples of $3\omega_B$ are bidirectional irrespective of σ_s .



As is seen in Figs. 5(a-b), when $\sigma_s < \sigma_{s,TH,1}$, the group velocity of a Bloch wave propagating from left to right (or right to left) approaches ∞ (or $-\infty$) when ω approaches certain values ω_p , which depend on the exact value of σ_s (p denotes positive integers). The group velocity is not definable exactly at ω_p . The values ω_{2q-1} and ω_{2q} both approach $\Omega_q = (q-1/2)3\omega_B$ when σ_s approaches $\sigma_{s,TH,1}$ (q denotes positive integers). As is seen in Fig. 6(c), when σ_s is around $\sigma_{s,TH,1}$, the phase of the transmission coefficient for the finite structure in Fig. 2(d) is almost uniform within a broad bandwidth ($\approx \omega_B$) around Ω_q , and as a result, the velocity v_T (defined above) has a very large absolute value within the bandwidth. According to

Fig. 6(d), v_T is equal to $118v_m$ at Ω_1 , where v_m denotes the speed of light in a medium of the refractive index n_m . The superluminal tunneling at Ω_q is ideal, because within the broad bandwidth, (i) R_L is almost zero, and (ii) $|T|$ is almost unity.



We note that this superluminal tunneling is bidirectional, because R_L and R_R are both zero at Ω_q . However, we prefer illuminating the structure from the left, because it yields a broader bandwidth. We also note that the behavior of the reflection zeros at Ω_q is similar to the behavior of those at the Dirac points and ESIBs; they are bidirectional irrespective of σ_s . In fact, the Dirac points and ESIBs (which turn into each other by changing σ_s) together with the states at $\omega = \Omega_q$ (which we name ‘turning points’) are the fixed points of the band structure. Given the Bloch wavenumbers equal to $\pm\pi/(2\Lambda)$ at the turning points, we expect that the electric field magnitude in the finite structure at Ω_q will be periodic irrespective of the illumination direction and σ_s . This prediction is confirmed by the numerical results in Figs. 5(g-h).

Concluding Remarks.— After a very brief review of important points about the PT-symmetric tight-binding models, we introduced novel band-structure concepts, such as ‘fixed points’ and ‘turning points’, in PT-symmetric non-tight-binding EM models. The resulting novel phenomena reported in this Letter included (i) the emergence of what we named ‘extended states

in the bandgap’ as the dual of ‘bound states in the continuum’, (ii) the enhancement of the EM fields at specific frequencies within specific regions, (iii) ‘bidirectional’ reflection zeros, and (iv) ‘ideal’ superluminal tunneling with zero reflection and a transmission coefficient of uniform phase and unit magnitude over a broad bandwidth. A quantum-optical treatment of these phenomena as well as the inclusion of nonlinear effects remains a subject for future work. Also, finding the electronic counterparts of the non-tight-binding EM structures examined here is another interesting problem. The band-structure concepts introduced in this Letter might be useful in designing other EM and electronic structures.

The author is deeply indebted to Prof. Behzad Rejaei for reviewing this Letter as well as being generous with his invaluable and insightful knowledge in the past few years.

- [1] C. W. Hsu, B. Zhen, A. D. Stone, J. D. Joannopoulos, and M. Soljačić, *Nat. Rev. Mater.* 1, 1 (2016).
- [2] S. Longhi, *Opt. Lett.* 39, 1697 (2014).
- [3] Y. Kartashov, C. Milián, V. V. Konotop, and L. Torner, *Opt. Lett.* 43, 575 (2018).
- [4] Q. Song, J. Hu, S. Dai, C. Zheng, D. Han, J. Zi, Z. Q. Zhang, and C. T. Chan, *Sci. Adv.* 6, eabc1160 (2020).
- [5] D. V. Novitsky, A. S. Shalin, D. Redka, V. Bobrovs, and A. V. Novitsky, *Phys. Rev. B* 104, 085126 (2021).
- [6] A. D. Stone, W. R. Sweeney, C. W. Hsu, K. Wisal, and Z. Wang, *Nanophotonics* 10, 343 (2021).
- [7] C. Spielmann, R. Szipöcs, A. Stingl, and F. Krausz, *Phys. Rev. Lett.* 73, 2308 (1994).
- [8] S. Longhi, M. Marano, P. Laporta, and M. Belmonte, *Phys. Rev. E* 64, 055602 (2001).
- [9] S. Manipatruni, P. Dong, Q. Xu, and M. Lipson, *Opt. Lett.* 33, 2928 (2008).
- [10] H. G. Winful, *Phys. Rev. Lett.* 90, 023901 (2003).
- [11] M. Büttiker and S. Washburn, *Nature* 422, 271 (2003).
- [12] R. Y. Chiao, P. G. Kwiat, and A. M. Steinberg, *Sci. Am.* 269, 52 (1993).
- [13] H. G. Winful, *Phys. Rep.* 436, 1 (2006).
- [14] Y. Liu, F. Sun, Y. Yang, Z. Chen, J. Zhang, S. He, and Y. Ma, *Phys. Rev. Lett.* 125, 207401 (2020).
- [15] P. A. Gusikhin, V. M. Muravev, and I. V. Kukushkin, *Phys. Rev. B* 102, 121404 (2020).
- [16] T. Low, P. Y. Chen, and D. N. Basov, *Phys. Rev. B* 98, 041403 (2018).
- [17] L. J. Wang, A. Kuzmich, and A. Dogariu, *Nature* 406, 277 (2000).
- [18] Q. Li, T. Wang, Y. Su, M. Yan, and M. Qiu, *Opt. Exp.* 18, 8367 (2010).
- [19] K. V. Klitzing, G. Dorda, and M. Pepper, *Phys. Rev. Lett.* 45, 494 (1980).
- [20] D. J. Thouless, M. Kohmoto, M. P. Nightingale, and M. den Nijs, *Phys. Rev. Lett.* 49, 405 (1982).
- [21] F. D. M. Haldane, *Phys. Rev. Lett.* 61, 2015 (1988).
- [22] Z. Wang, Y. D. Chong, J. D. Joannopoulos, and M. Soljačić, *Phys. Rev. Lett.* 100, 013905 (2008).
- [23] C. L. Kane and E. J. Mele, *Phys. Rev. Lett.* 95, 226801 (2005).
- [24] B. A. Bernevig, T. L. Hughes, and S. C. Zhang, *Science* 314, 1757 (2006).
- [25] M. König, S. Wiedmann, C. Brune, A. Roth, H. Buhmann, L. W. Molenkamp, X. L. Qi, and S. C. Zhang, *Science* 318, 766 (2007).
- [26] M. Hafezi, S. Mittal, J. Fan, A. Migdall, and J. M. Taylor, *Nat. Photon.* 7, 1001 (2013).
- [27] A. B. Khanikaev, S. H. Mousavi, W. K. Tse, M. Kargarian, A. H. MacDonald, and G. Shvets, *Nat. Mater.* 12, 233 (2013).
- [28] W. P. Su, J. R. Schrieffer, and A. J. Heeger, *Phys. Rev. Lett.* 42, 1698 (1979).
- [29] F. K. Kunst, E. Edvardsson, J. C. Budich, and E. J. Bergholtz, *Phys. Rev. Lett.* 121, 026808 (2018).
- [30] W. Song, W. Sun, C. Chen, Q. Song, S. Xiao, S. Zhu, and T. Li, *Phys. Rev. Lett.* 123, 165701 (2019).
- [31] S. Yao and Z. Wang, *Phys. Rev. Lett.* 121, 086803 (2018).

- [32] C. M. Bender and S. Boettcher, *Phys. Rev. Lett.* 80, 5243 (1998).
- [33] H. Schomerus, *Opt. Lett.* 38, 1912 (2013).
- [34] S. Weimann, M. Kremer, Y. Plotnik, Y. Lumer, S. Nolte, K. G. Makris, M. Segev, M. C. Rechtsman, and A. Szameit, *Nat. Mater.* 16, 433 (2017).
- [35] S. Ke, D. Zhao, J. Liu, Q. Liu, Q. Liao, B. Wang, and P. Lu, *Opt. Exp.* 27, 13858 (2019).
- [36] S. K. Özdemir, S. Rotter, F. Nori, and L. Yang, *Nat. Mater.* 18, 783 (2019).
- [37] M. Kulishov, J. M. Laniel, N. Bélanger, J. Azaña, and D. V. Plant, *Opt. Exp.* 13, 3068 (2005).
- [38] Z. Lin, H. Ramezani, T. Eichelkraut, T. Kottos, H. Cao, and D. N. Christodoulides, *Phys. Rev. Lett.* 106, 213901 (2011).
- [39] K. Sakoda, *Optical properties of photonic crystals*. (Springer Science & Business Media, 2004).
- [40] S. Buddhiraju, A. Song, G. T. Papadakis, and S. Fan, *Phys. Rev. Lett.* 124, 257403 (2020).
- [41] M. Farhat, M. Yang, Z. Ye, and P. Y. Chen, *ACS Photonics* 7, 2080 (2020).
- [42] M. Born and E. Wolf, *Principles of optics: electromagnetic theory of propagation, interference and diffraction of light* (Elsevier, 2013).